

## Numerical analysis of injection molding for filling efficiency on ultrasonic process

Jaeyeol Lee<sup>1</sup>, Naksoo Kim<sup>1,\*</sup> and Jaewook Lee<sup>2</sup>

<sup>1</sup>Department of Mechanical Engineering, Sogang University, Seoul 121-742, Korea

<sup>2</sup>Department of Chemical and Biomolecular Engineering, Sogang University, Seoul 121-742, Korea

(Received February 19, 2008; final revision received May 2, 2008)

### Abstract

In this study, we focus on the improvement of the filling efficiency in injection molding by application of ultrasonic vibration. While studies about the filling efficiency of typical filling processes in the injection molding have been widely performed, there have been only few studies about the filling efficiency of an ultrasonic process. The effect of the ultrasonic vibration is an important process condition, which influences the flow characteristics of polymer melt. This new condition even affects well-known injection conditions such as cavity pressure, injection temperature and mold temperature. For this study, we carried out a numerical analysis by appropriate modeling and analysis of the ultrasonic process in the filling process. To verify this numerical analysis, we compared the numerical results with the experimental data. Also, we analyzed the filling process in a thin cavity using this numerical analysis. To understand the flow characteristics of polymer melt in the ultrasonic process, we substituted real and complex vibration conditions with simplified and classified conditions according to the position of vibrating cavity surfaces and the phase difference between two opposing cavity surfaces. We also introduced MFR (melt flow ratio) as a new index to estimate the filling efficiency in the ultrasonic process.

**Keywords** : polymer, ultrasonic, vibration, flow rate, filling process, injection molding, efficiency

### 1. Introduction

In recent polymer consumption, the demand for thin and light-weighted products has been increasing. On the other hand, the short-shot problem during the manufacturing of these products often occurs due to the high viscosity characteristics of polymer melt. Short-shot means that not enough polymer melt has flowed into a cavity to fill it adequately. For solving this problem, an ultrasonic process is applied to the filling process of injection molding.

Chen and Li (2006; 2007), Zhang *et al.* (2006) concluded that low injection pressure and high flow rate are obtained because of ultrasonic vibration, when polymer melt is injected into a thin and wide cavity. Feng and Isayev (2004), Swain and Isayev (2007) determined the relationship between the intensity and the amplitude of ultrasonic vibration by an experimental study. They studied not only the variation of injection pressure according to the amplitude but also stress-strain curve as the mechanical property. Ho *et al.* (1993) performed researches about variations of mechanical properties owing to the ultrasonic vibration on polymer melt mixing. Mechanical properties of FRP (fiber reinforced plastics) affected by an ultrasonic process were

also studied by Morii *et al.* (1999).

From the standpoint of flow physics, ultrasonic vibration affects two primary factors of polymer melt. They are typically the viscosity and the molecular weight. Kim *et al.* (2002) carried out an experimental study on the variations of the viscosity of polymer melt according to the ultrasonic frequency, the ultrasonic exposure time, mixing temperature and the rotor speed in the extrusion process. Madras *et al.* (2000) studied the variation of the molecular weight of polymer melt due to the effect of the ultrasonic vibration by experiments. Kanwal *et al.* (2000) concluded that the ultrasonic exposure time caused the decrease of the molecular weight as well as variations of mechanical properties. Li *et al.* (2005) studied the decreases of both viscosity and molecular weight of two polymer melts (polystyrene and ethylene-propylene diene monomer) according to the ultrasonic exposure time and intensity.

In addition, Price *et al.* (2002) studied not only the variation of the molecular weight, but also the melting point of polymer melt due to the effect of ultrasonic vibration. Sahnoune and Piche (1998) carried out an experimental study on the thermal property of polymer melt such as the thermal expansivity. Shim *et al.* (2002) studied the number and diameter of bubbles in polymer melt according to the ultrasonic vibration intensity and applied pressure by experiments.

On the other hand, many numerical analyses were carried

\*Corresponding author: nskim@sogang.ac.kr  
© 2008 by The Korean Society of Rheology

out to predict the behavior of polymer melt in injection molding. Kim *et al.* (2006a; 2006b), Ye *et al.* (2005) performed a numerical analysis about the behavior of polymer melt in the extrusion system using FVM (finite volume method). To predict the growth of bubble in polymer melt owing to the effect of the ultrasonic vibration, Park *et al.* (1995), Youn (1999) and Koo *et al.* (2001) carried out a numerical study. Mousavi *et al.* (2007) also investigated a numerical analysis to predict the extrusion force due to ultrasonic vibration.

In order to verify the validity of our numerical analysis, we compared the numerical results with the experimental data of Chen and Li (2006). Next, we also modeled the injection of polymer melt into a thin and wide cavity and analyzed the variations of the filling efficiency according to the injection conditions (cavity pressure, injection temperature and mold temperature) and vibration conditions (amplitude, frequency, position of vibrating cavity surfaces and phase difference between two vibrations). Ultimately, we aimed to find more efficient process conditions in the ultrasonic process.

## 2. Theory

### 2.1. Ultrasonic vibration

A piezoelectric transducer generates ultrasonic vibration from applied AC (alternating current). An ultrasonic horn is a device used to amplify this vibration. As a result, polymer melt in the cavity is filled with the effect of this ultrasonic vibration as shown in Fig. 1.

When the ultrasonic vibration is propagated, the vibrational energy in a unit area vertical to the direction of propagation is as follows:

$$I = 2\pi^2 \rho c f^2 x^2 = A f^2 x^2, \quad (1)$$

where  $\rho$  is the density of the material,  $c$  is the propagation velocity of the ultrasonic vibration,  $f$  is the frequency of the ultrasonic vibration and  $x$  is the amplitude. The frequency of the ultrasonic vibration is 20 kHz or more. Therefore, the intensity of ultrasonic vibration is very high.

### 2.2. Governing equation

Polymer melt is generally a non-Newtonian fluid. Its

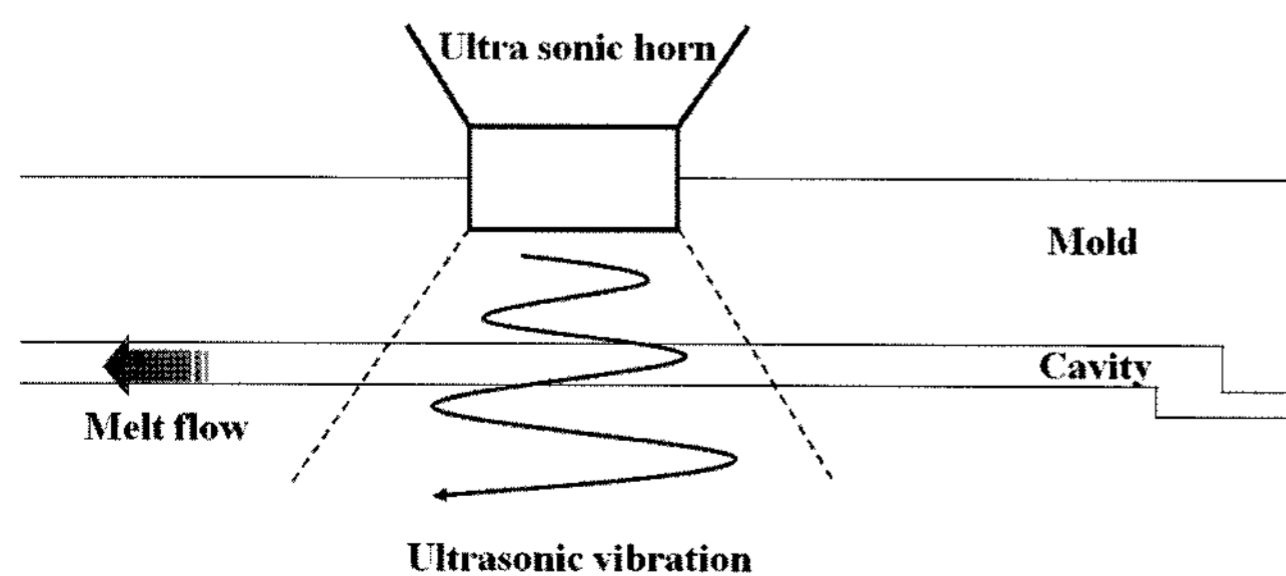


Fig. 1. Application of ultrasonic vibration in injection molding.

flow characteristics are incompressible and laminar. To express these flow characteristics in the Cartesian coordinate system, the continuity and the momentum equations are given as follows:

$$\frac{\partial \rho}{\partial t} + \frac{\partial}{\partial x_j}(\rho u_j) = s_m, \quad (2)$$

$$\frac{\partial(\rho u_i)}{\partial t} + \frac{\partial}{\partial x_j}(\rho u_j u_i - \tau_{ij}) = -\frac{\partial p}{\partial x_i} + s_i, \quad (3)$$

$$\frac{\partial(\rho h)}{\partial t} + \frac{\partial}{\partial x_j}(\rho h u_j + F_{h,j}) = \frac{\partial p}{\partial t} + u_j \frac{\partial p}{\partial x_j} + \tau_{ij} \frac{\partial u_i}{\partial x_j} + s_h. \quad (4)$$

In this study, these equations are calculated using the PISO (pressure implicit with splitting of operators) algorithm in FVM. The flux term is solved by the upwind scheme. The shear stress is expressed by the following constitutive law.

$$\tau_{ij} = 2\mu s_{ij} - \frac{2}{3}\mu \frac{\partial u_k}{\partial x_k} \delta_{ij}, \quad (5)$$

$$\text{where } s_{ij} = \frac{1}{2} \left( \frac{\partial u_i}{\partial x_j} + \frac{\partial u_j}{\partial x_i} \right).$$

### 2.3. Carreau-Yasuda model

The Carreau-Yasuda model is considered as a viscosity model. This model, which has functions of deformation rate and temperature, is expressed by equation (6). It is transformed to a user subroutine in the FVM calculation.

$$\mu = \mu_0 \alpha [1 + (\lambda \dot{\gamma})]^{(n-1)/2}, \quad (6)$$

$$\alpha = \exp \left[ \beta \left( \frac{1}{T} - \frac{1}{T_{ref}} \right) \right],$$

$$\text{and } \dot{\gamma} = \sqrt{\frac{1}{2}(s_{ij}s_{ij} - s_{ii}s_{jj})},$$

where  $\alpha$  is the temperature shift and  $\dot{\gamma}$  is the deformation rate. In general, the reference temperature  $T_{ref}$  is 473.15 K. These constants are shown in Table 1. The viscosity decreases with the increase of the deformation rate in equation (6).

To investigate the flow rate according to the viscosity

Table 1. Viscosity model of polymer melt

	Viscosity model		
	LDPE	PP	PS
Power-law index, $n$ [Pa-sec <sup>n</sup> ]	0.61	0.43	0.66
Temperature sensitivity, $\beta$ [K]	6330	6731	5200
Time constant, $\lambda$ [sec]	0.28	0.13	0.64
Zero shear strain viscosity, $\mu_0$ [Pa-sec]	5645	3523	2410

**Table 2.** Properties of polymer melt

	Physical properties		
	LDPE	PP	PS
Density [kg/m <sup>3</sup> ]	920	905	1060
Heat capacity [J/kg·K]	2780	1930	1200
Conductivity [W/m·K]	0.21	0.24	0.12

characteristics, LDPE (low density polyethylene), PP (polypropylene) and PS (polystyrene) are considered in this study.

#### 2.4. Deformation rate and viscosity

The deformation rate, which has functions of elongation rate and shear rate, is expressed by equation (7). The elongation rate is expressed by the first three terms in equation (7), while the shear rate is represented by the last three terms.

$$|\dot{\gamma}(t)| = \left[ \begin{array}{l} 2\left(\frac{\partial u}{\partial x}\right)^2 + 2\left(\frac{\partial v}{\partial y}\right)^2 + 2\left(\frac{\partial w}{\partial z}\right)^2 \\ + \left(\frac{\partial v}{\partial x} + \frac{\partial u}{\partial y}\right)^2 + \left(\frac{\partial w}{\partial y} + \frac{\partial v}{\partial z}\right)^2 + \left(\frac{\partial u}{\partial z} + \frac{\partial w}{\partial x}\right)^2 \end{array} \right]^{\frac{1}{2}} \quad (7)$$

### 3. Verification of the numerical analysis

#### 3.1. Geometry and material properties

Chen and Li (2006) carried out an experimental study about the application of ultrasonic vibration in the filling process. In their study, they concluded that the flow rate of PS increases with the increase of ultrasonic vibration intensity. To verify the validity of our numerical analysis, we compared the numerical results with the experimental data of Chen and Li (2006).

In this study, we numerically analyzed the flow characteristics of polymer melt in the filling process using a commercial code, STAR-CD, based on FVM. As a physical phenomenon, vibrations on the cavity surfaces, produced by the ultrasonic vibration, were applied to the velocity and wall boundary conditions using the moving grid method. Also, we found that there was no further improvement of the filling efficiency with longer than the time period of the ultrasonic vibration, 0.01 second, while the efficiency significantly improved with less than the time period of the ultrasonic vibration, 0.01 second. Therefore, we decided that the time period of the ultrasonic vibration is good enough with 0.01 seconds.

Fig. 2(a) shows the geometry of the extrusion system, which was used in the experimental study by Chen and Li (2006). Based on this geometry, Fig. 2(b) shows the analysis domain, which was modeled in our numerical study using FVM.

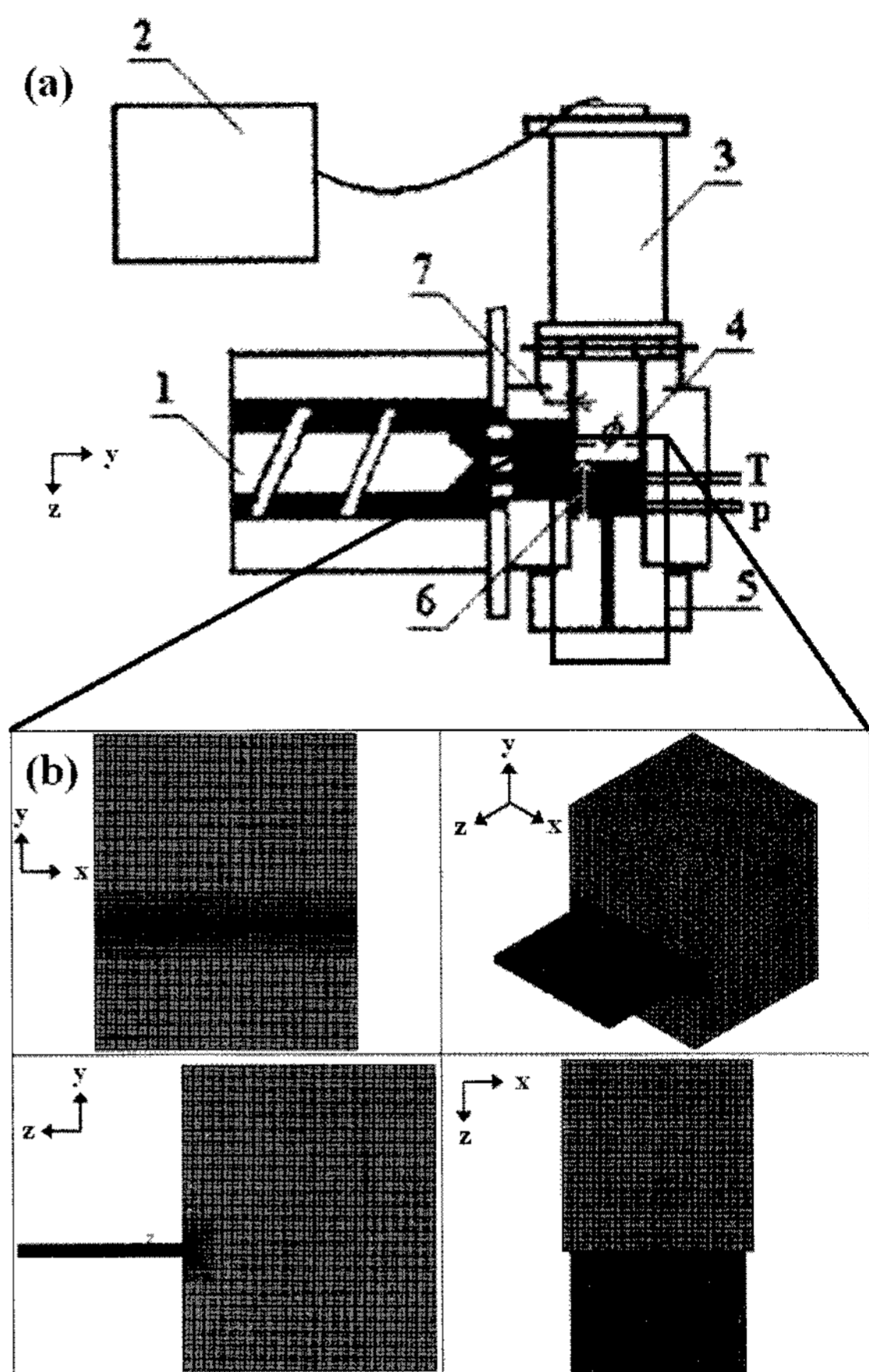


**Fig. 2.** Geometry of the extrusion system; (a) geometry in the experimental study by Chen and Li (2006): 1, extruder; 2, ultrasonic generator; 3, piezoelectric transducer; 4, diameter of the ultrasonic horn is 10 mm; 5, mold; 6, gap between the horn and the entrance to the cavity is 10 mm; 7, gap between the horn and the mold is 1 mm, (b) geometry of the analysis domain.

As shown in Table 2, the material properties of LDPE, PP and PS were assigned as constant values in this study.

#### 3.2. Results and discussions

The numerical results were compared with the experimental data of Chen and Li (2006) to verify our numerical analysis in Fig. 3. The flow rate increased with the increase of the ultrasonic intensity and cavity pressure.

In the case of 0 W, there was little difference between the numerical results and the experimental data. On the other hand, as both cavity pressure and the ultrasonic intensity increased, the numerical results showed differences with the experimental data. These reasons are that the variations of the density and the heat capacity of polymer melt according to applied pressure, the generation of the cavitation due to the phase change of polymer melt and the effect of the modeling error were not considered.

But on the whole, the pattern of the numerical results was similar to that of the experimental data. In conclusion,

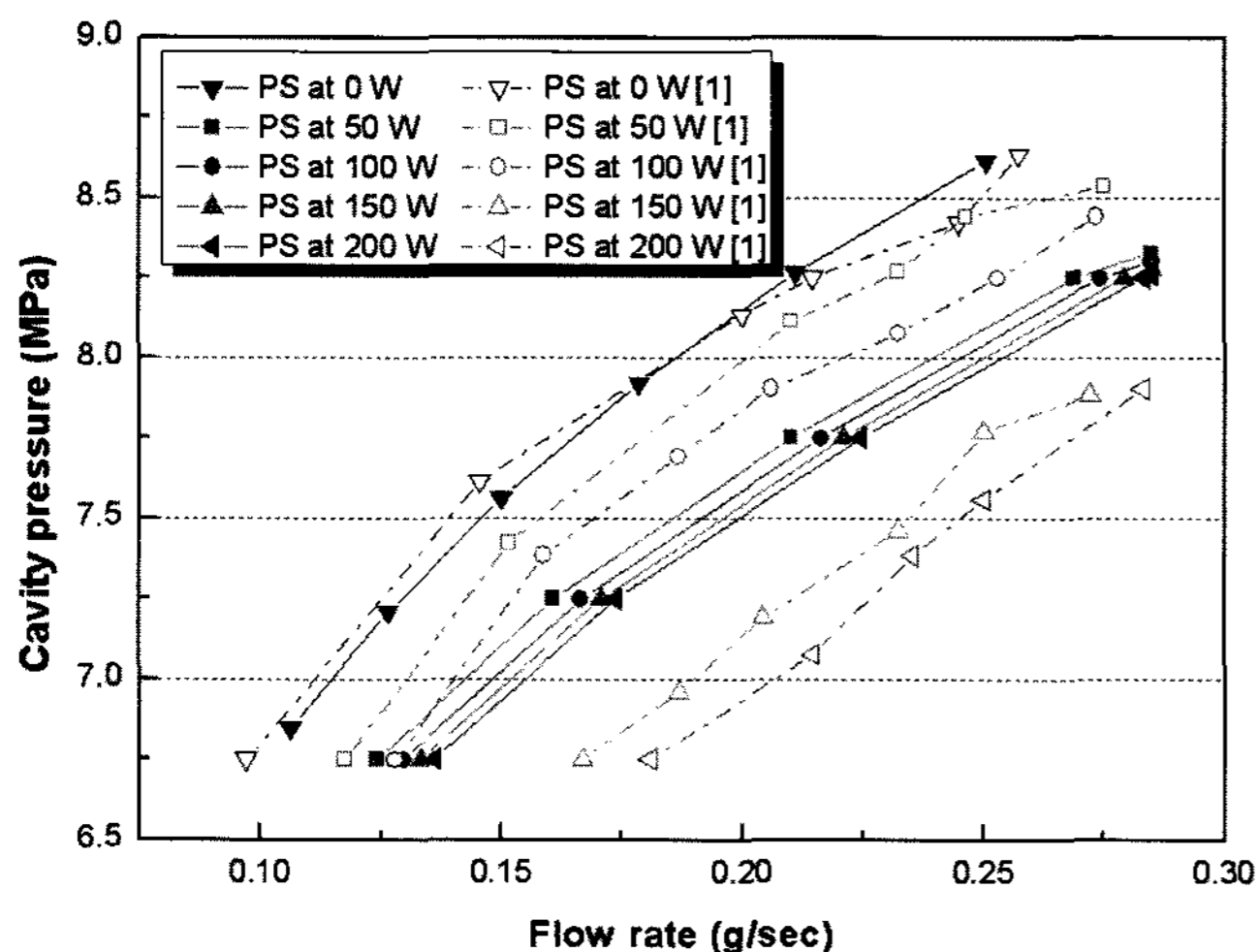
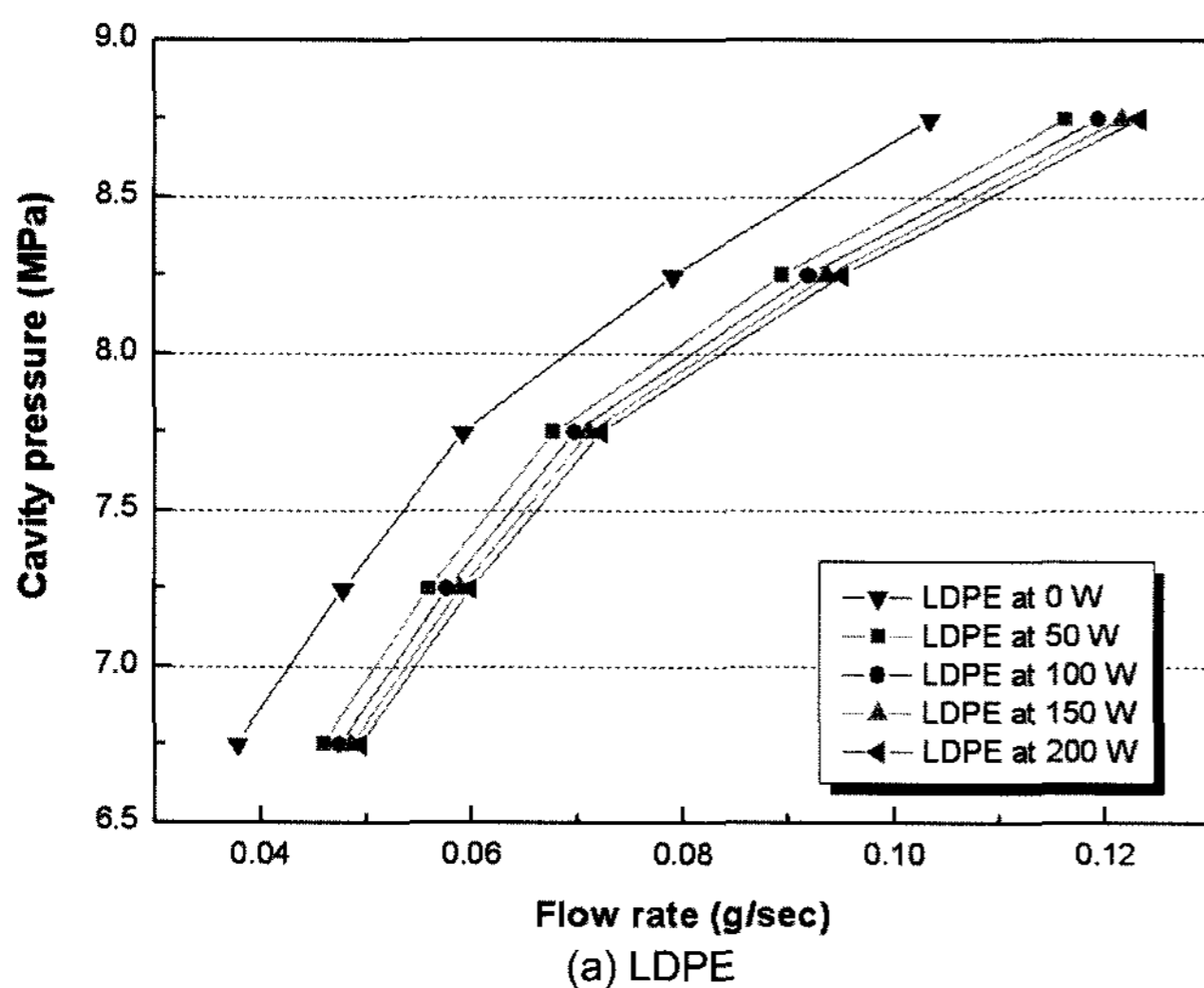
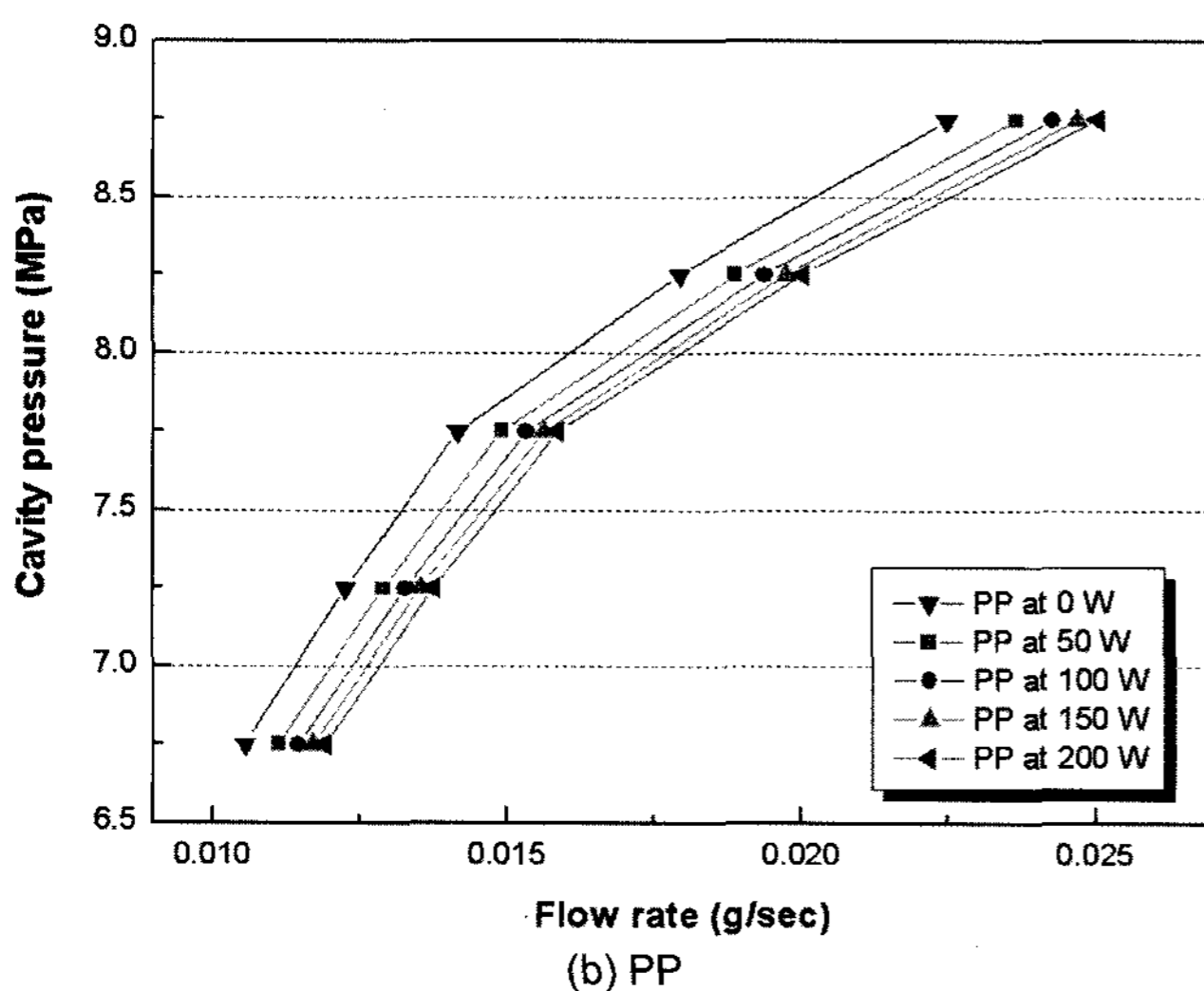


Fig. 3. Comparison of numerical result with experimental data of Chen and Li (2006).



(a) LDPE



(b) PP

Fig. 4. Variation of flow rate according to cavity pressure for various intensities; (a) LDPE, (b) PP.

this numerical analysis was a valid method for analyzing the effect of the ultrasonic vibration in the filling process.

In Fig. 4, we analyzed the flow rates of LDPE and PP obtained using this numerical analysis according to the intensity of the ultrasonic vibration and cavity pressure. Although the numerical analysis and the boundary conditions were the same, there were significant differences of the flow rate between two polymer melts. This reason is that the viscosity characteristics of the polymer materials are different each other.

In conclusion, the flow rate of polymer melt increased with the ultrasonic intensity or cavity pressure increased. Also, there were differences of the flow rate between each polymer melt.

#### 4. Filling efficiency according to injection conditions

##### 4.1. MFR (melt flow ratio)

In this study, we used a new index for the estimation of the filling efficiency affected by the application of the ultrasonic vibration in the filling process. This new index is as follows:

$$\text{MFR (melt flow ratio)} = \frac{\dot{m}_{uv}}{\dot{m}_0}, \quad (8)$$

where  $\dot{m}_{uv}$  and  $\dot{m}_0$  are the flow rate with and without the ultrasonic vibration, respectively. For example, when flow rate increases due to the effect of the ultrasonic vibration, MFR (melt flow ratio) also increases. On the contrary, with no effect of the ultrasonic vibration, MFR value is one. In other words, the filling efficiency is zero. In general, the flow rate with the ultrasonic vibration is higher than that without the vibration. Therefore, the value of MFR is higher than one.

##### 4.2. Geometry of the cavity

Fig. 5 shows the thin and wide cavity ( $200 \times 20 \times 2 \text{ mm}^3$ ) model used to analyze the filling efficiency with the ultrasonic vibration. Polymer melt at the inlet is injected into the cavity. After it passes through the vibration region which is generated by the ultrasonic vibration, it goes out of the cavity through the outlet. The vibration region, composed of a total of four cavity surfaces, is assumed so that the only a specific region of the cavity surfaces is oscillated by the vibration of the ultrasonic horn, as shown in Fig. 1.

To analyze the filling efficiency according to injection conditions, we considered that two opposing cavity surfaces in the y-direction are vibrated with the phase difference  $180^\circ$ . In other words, the upper and down cavity surfaces in the y-direction are vibrated with the phase difference  $180^\circ$  among the vibration region. The phase difference  $180^\circ$  means that the upper surface moves in the positive y-direction when the down surface moves in the

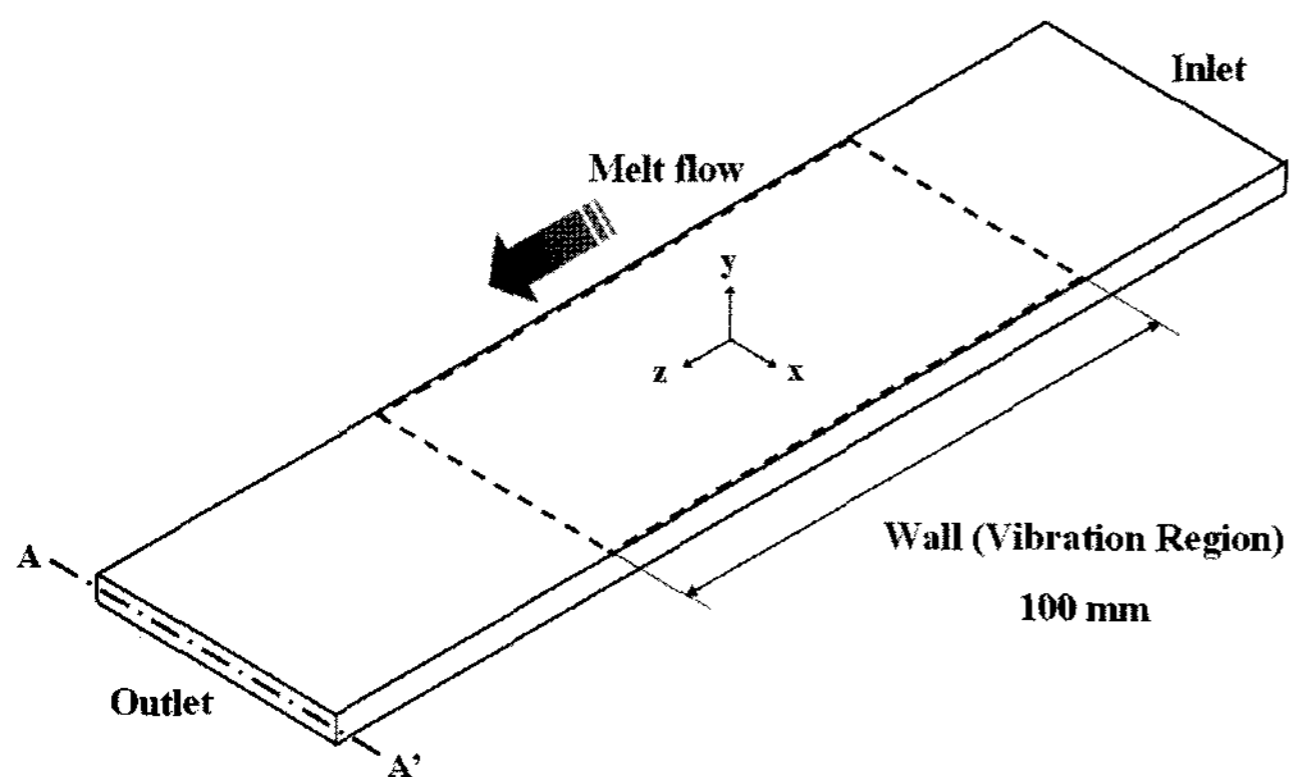


Fig. 5. Geometry and analysis domain of the cavity ( $200 \times 20 \times 2 \text{ mm}^3$ ).

negative y-direction.

Injection conditions, which are considered in this paper, consist of cavity pressure, mold temperature, injection temperature and the thickness of the cavity. Cavity pressure and injection temperature mean the relative pressure from the inlet to the outlet and the absolute temperature of the injected polymer melt into the cavity, respectively. Mold temperature represents the absolute temperature of the cavity surfaces.

If the boundary conditions are not separately mentioned in this study, injection conditions are constant values as follows: cavity pressure is 60 MPa, mold temperature, 323.15 K, and injection temperature, 473.15 K.

The filling efficiency of polymer melt is related to its viscosity characteristics, caused by the ultrasonic vibration. So, we considered PP as a low viscosity material, whereas LDPE was considered as a high viscosity material in this study.

#### 4.3. Results and discussions

Fig. 6 shows the variation of MFR according to cavity pressure at 100 W. MFR decreases with the increase of cavity pressure. This result shows that the filling efficiency decreases with the increase of cavity pressure under the same vibration condition. As cavity pressure is 30 MPa or above, the filling efficiencies of both LDPE and PP remain almost the same with the increase of cavity pressure. In particular, MFR of LDPE is almost one when cavity pressure is 60 MPa. It can also explain that the filling efficiency of LDPE at 60 MPa is hardly affected by the ultrasonic vibration.

On the other hand, the filling efficiency of PP is higher than that of LDPE because the flow rate of PP is lower than that of LDPE under the same injection conditions, as shown in Fig. 4. Therefore, the ultrasonic vibration had a relatively stronger effect on the increase of the flow rate of PP rather than on that of LDPE.

The variation of the filling efficiency according to injection temperature was investigated by the MFR of both LDPE and PP at 100 W, as shown in Fig. 7. The MFR of

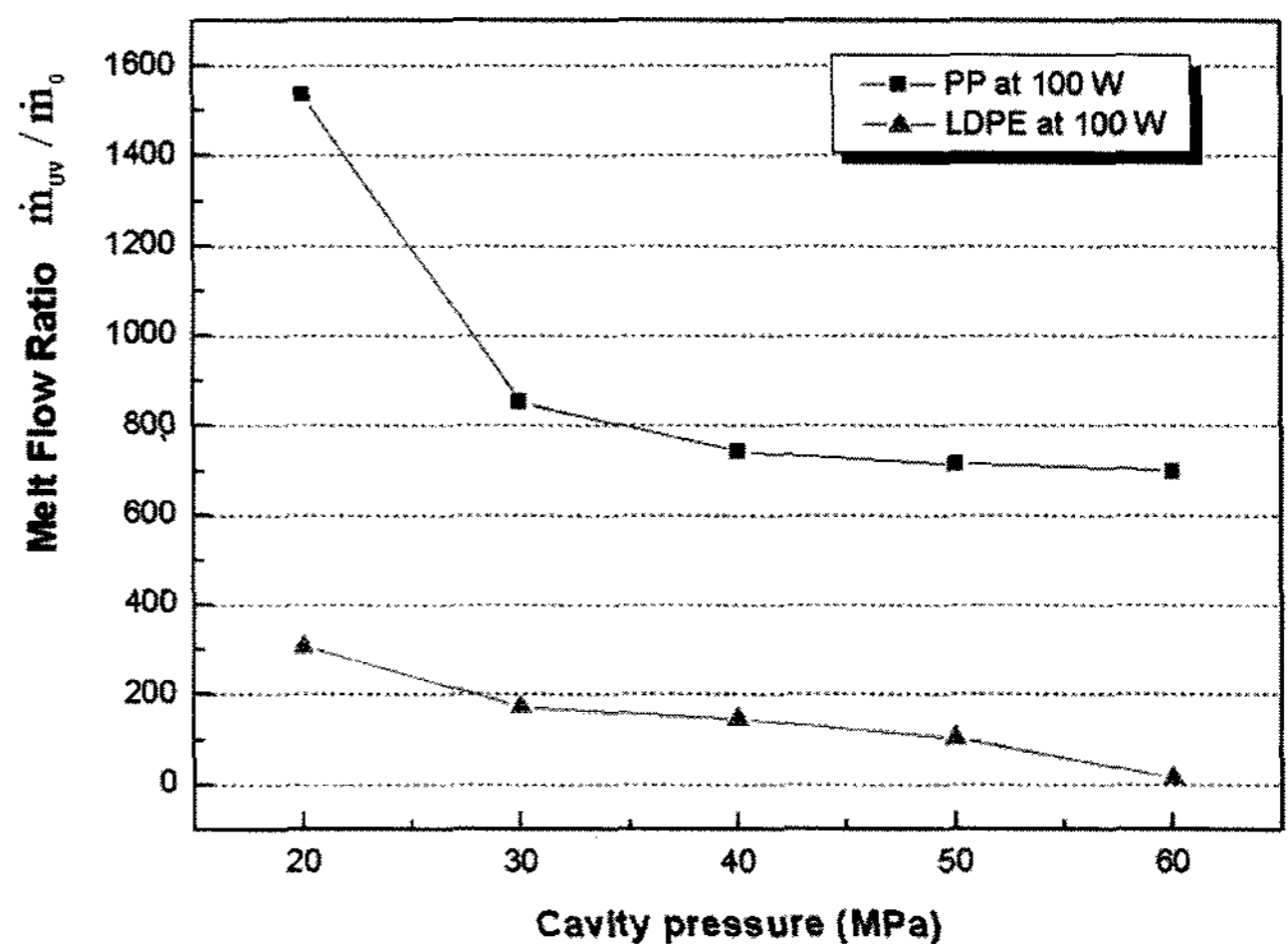


Fig. 6. Comparison of MFR according to cavity pressure.

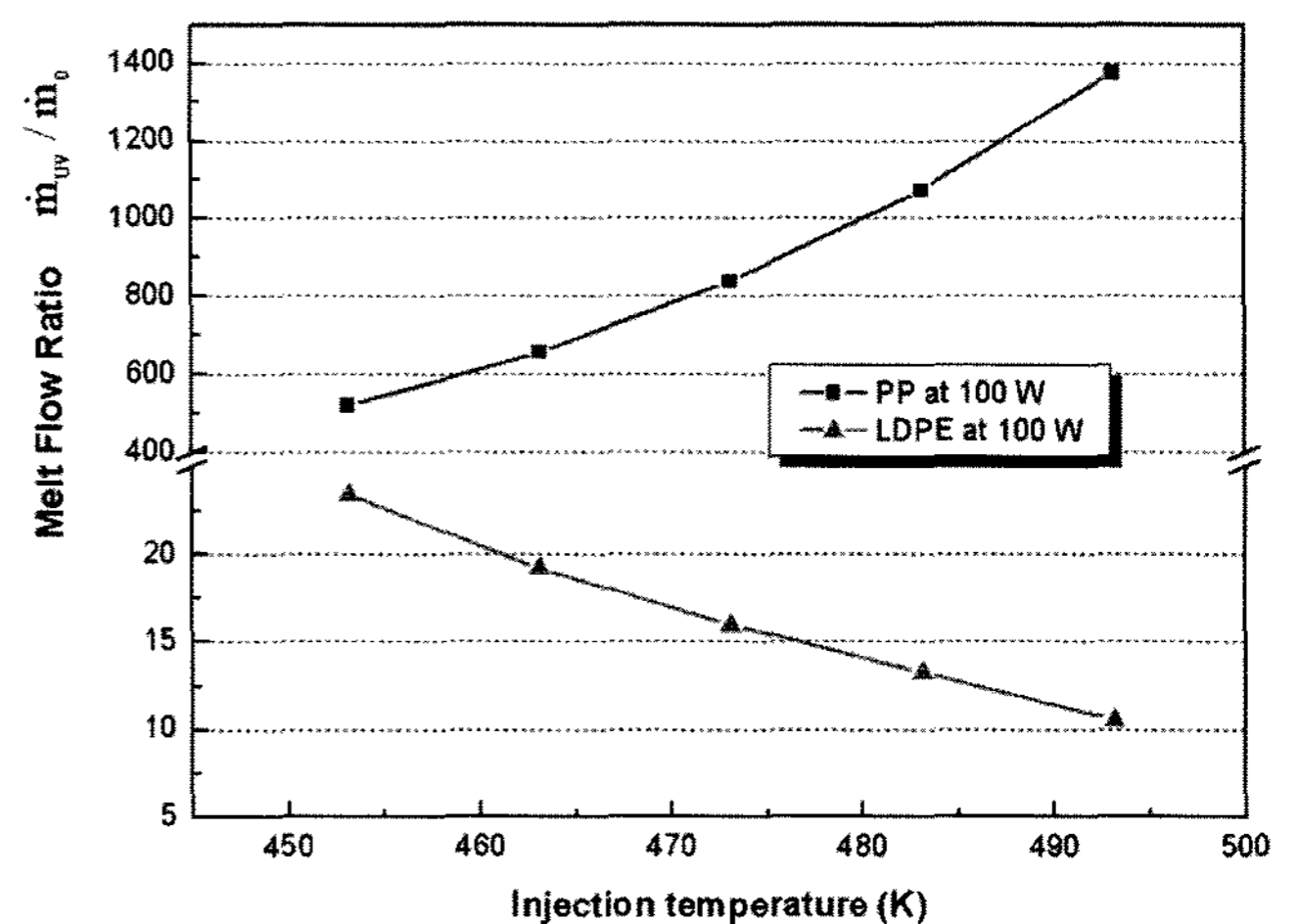


Fig. 7. Variation of MFR according to injection temperature.

LDPE decreases with the increase of injection temperature, whereas that of PP increases despite the same increase of injection temperature. In conclusion, if the flow rate is low such as PP, the filling efficiency increased with the increase of injection temperature. On the contrary, if the flow rate is high such as LDPE, the filling efficiency decreased with the same increase of injection temperature.

In the case of LDPE, the typical applied injection temperature ranged from 433.15 to 493.15 K and that of PP ranged from 453.15 to 493.15 K. The minimum injection temperature of 433.15 K yielded the most efficient condition in the case of LDPE, whereas the maximum temperature of 493.15 K yielded the most efficient condition in the case of PP.

Fig. 8 shows the variations of MFR according to mold temperature at 100 W. MFR decreases with the increase of mold temperature. As compared with the MFR of PP, the MFR of LDPE hardly changed according to mold temperature. The filling efficiency of polymer melt, which was obtained at relatively low flow rate like that of PP, drops

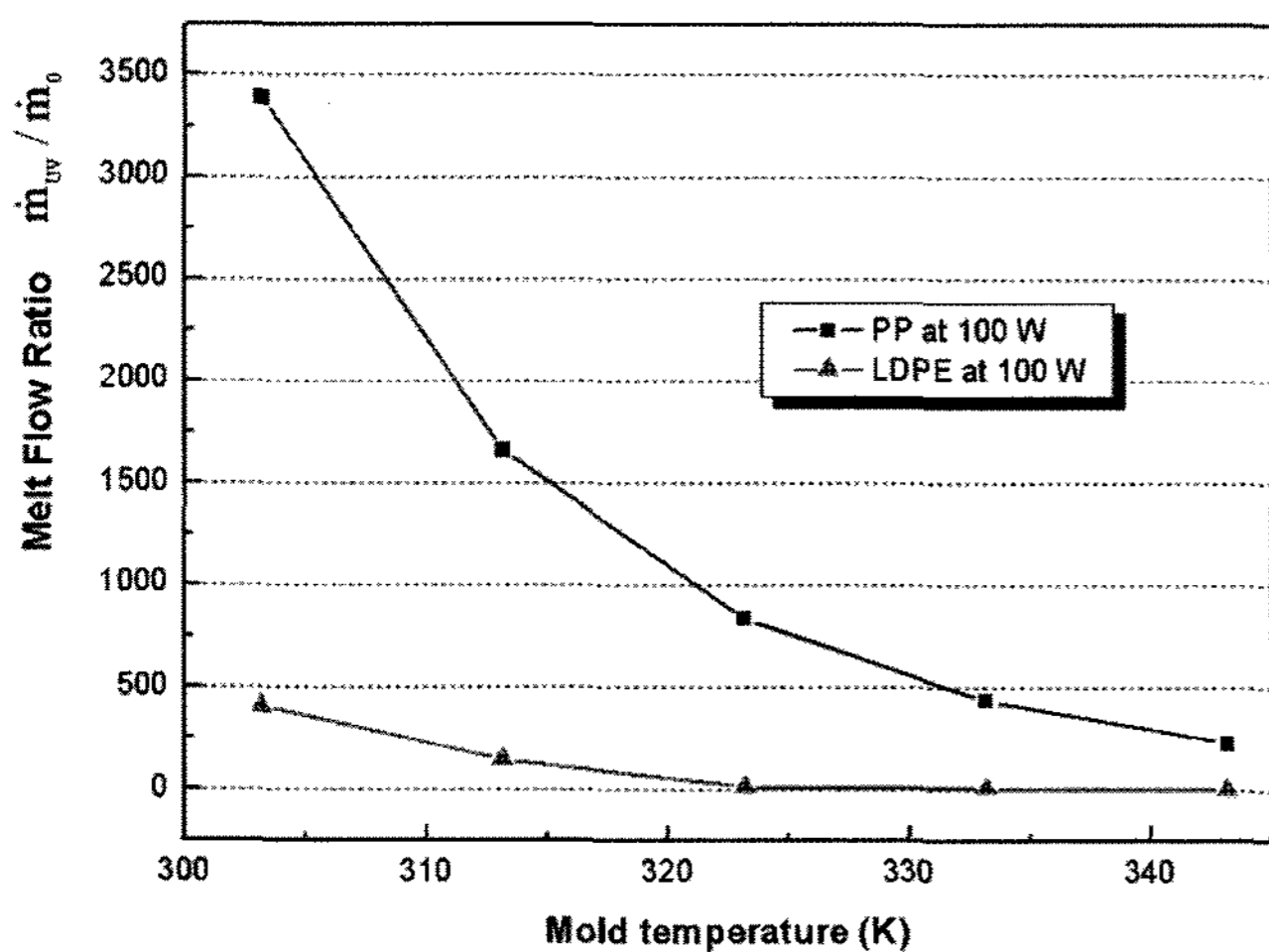


Fig. 8. Comparison of MFR according to mold temperature.

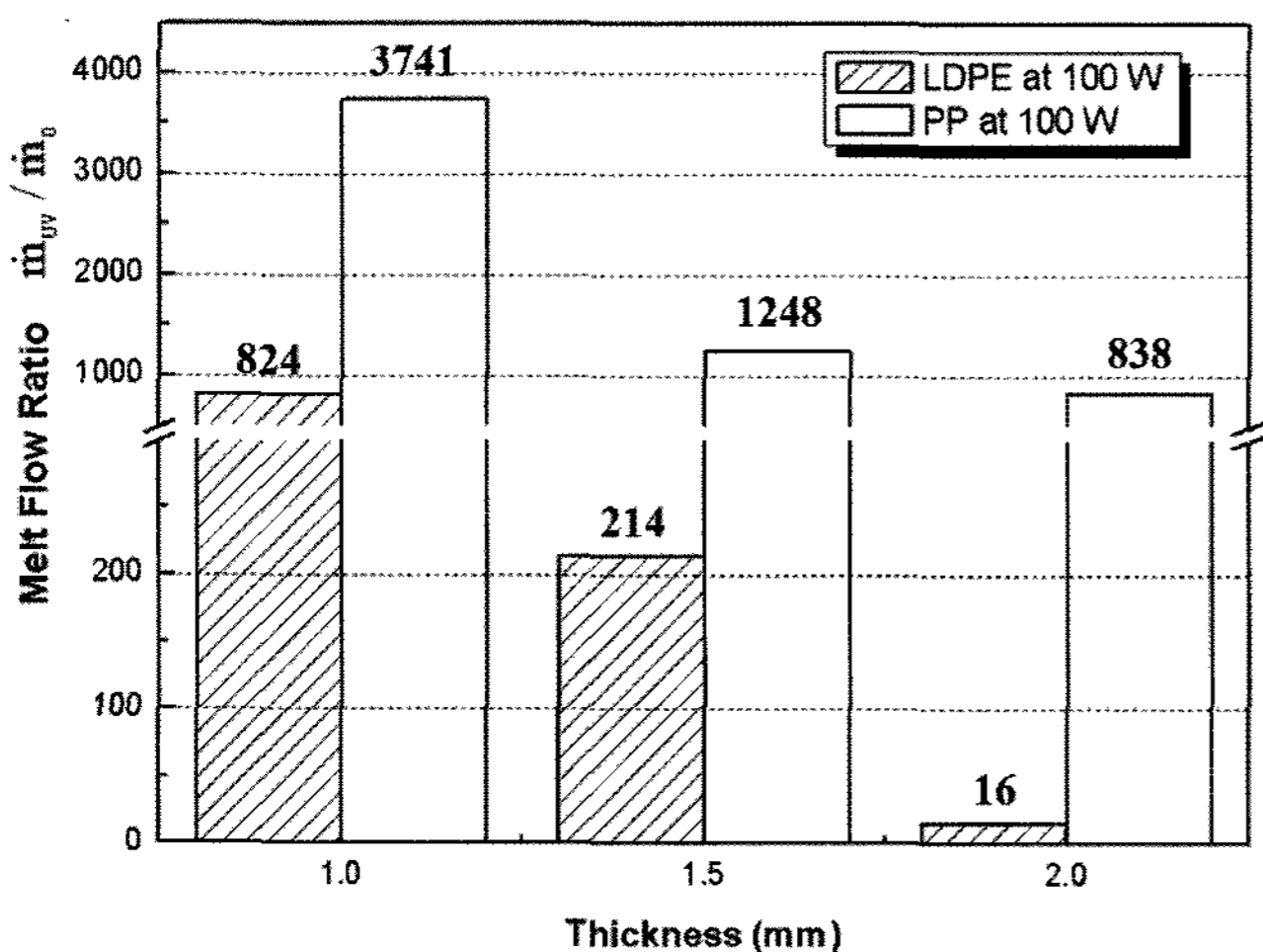


Fig. 9. Variation of MFR according to the thickness of the cavity.

rapidly with the increase of mold temperature owing to the effect of the ultrasonic vibration.

In the cases of both LDPE and PP, the typical range of the applied mold temperature is about from 303.15 to 323.15 K. Therefore, the difference between the filling efficiencies of LDPE and PP is expected to be large.

MFR according to a thickness of the cavity is shown in Fig. 9. This result, which is similar to the above result, shows that the filling efficiency of PP is higher than that of LDPE as a whole. MFR also decreases with the increase of the thickness at 100 W.

In the case of PP, when the thickness increased from 1.0 to 1.5 and 2.0 mm, the MFR decrease rate ranged from 66.64 to 32.85%, respectively. The MFR decrease rate means the rate of decrease of filling efficiency due to the difference between two thicknesses. On the other hand, the MFR decrease rate of LDPE ranged 74.03 to 92.52%, respectively. In other words, while the highest value of the MFR decrease rate of the case of PP was obtained when the cavity thickness was between 1.0 and 1.5 mm, that of

the case of LDPE was obtained when the thickness was between 1.5 and 2.0 mm.

In conclusion, the filling efficiency decreased with the increase of the cavity thickness. Also, the rate of decrease changed with material according to the cavity thickness under the same injection and vibration conditions.

## 5. Filling efficiency according to vibration conditions

When the ultrasonic vibration was applied, the primary physical phenomenon was the generation of vibrations on the cavity surfaces due to the mode shape of the cavity or mold. The mode shape means the spatial deformation of the structure owing to the effect of the vibration. The mold vibrates due to the effect of the ultrasonic horn, as shown in Fig. 1, according to the shape of mold vibration (or the mode shape). This effect of the mode shape vibrates the cavity surfaces. As a result, this vibration on the surfaces generates a vibration region, which has influence on polymer melt in the cavity, as shown in Fig. 5. In general, the mode shape is very complex and thus, vibration conditions are also complex. Such complexities make it hard to analyze the effect of each vibration condition. For this reason, the amplitude of the ultrasonic vibration on the cavity surfaces is characterized as a sine curve from end to end of the vibration region. The factors of vibration conditions are also classified so that the relationship between the frequency and the amplitude of vibration, the positions of vibrating cavity surfaces and the phase difference between two opposing cavity surfaces can be considered.

Table 3 shows the classification of vibration conditions. This classification can facilitate the understanding of the effect of each vibration condition. In CASE I, we analyzed of the MFR and the flow characteristics according to the positions of the vibrating cavity surfaces. Also, the phase difference of vibration between two opposing cavity surfaces in the vibration region is considered in CASE II.

### 5.1. Relationship between the frequency and the amplitude of vibration

The mode shape of the ultrasonic horn, which vibrates a cavity directly, is very dependent on the applied frequency. This is because the ultrasonic horn is designed to operate at a specified frequency (typically 20 kHz or more) to obtain maximum displacement and force. For this reason,

Table 3. Classification of vibration conditions

	CASE I	CASE II
Position of vibrating surfaces	x or y-direction	y-direction
Phase difference	180°	0 or 180°

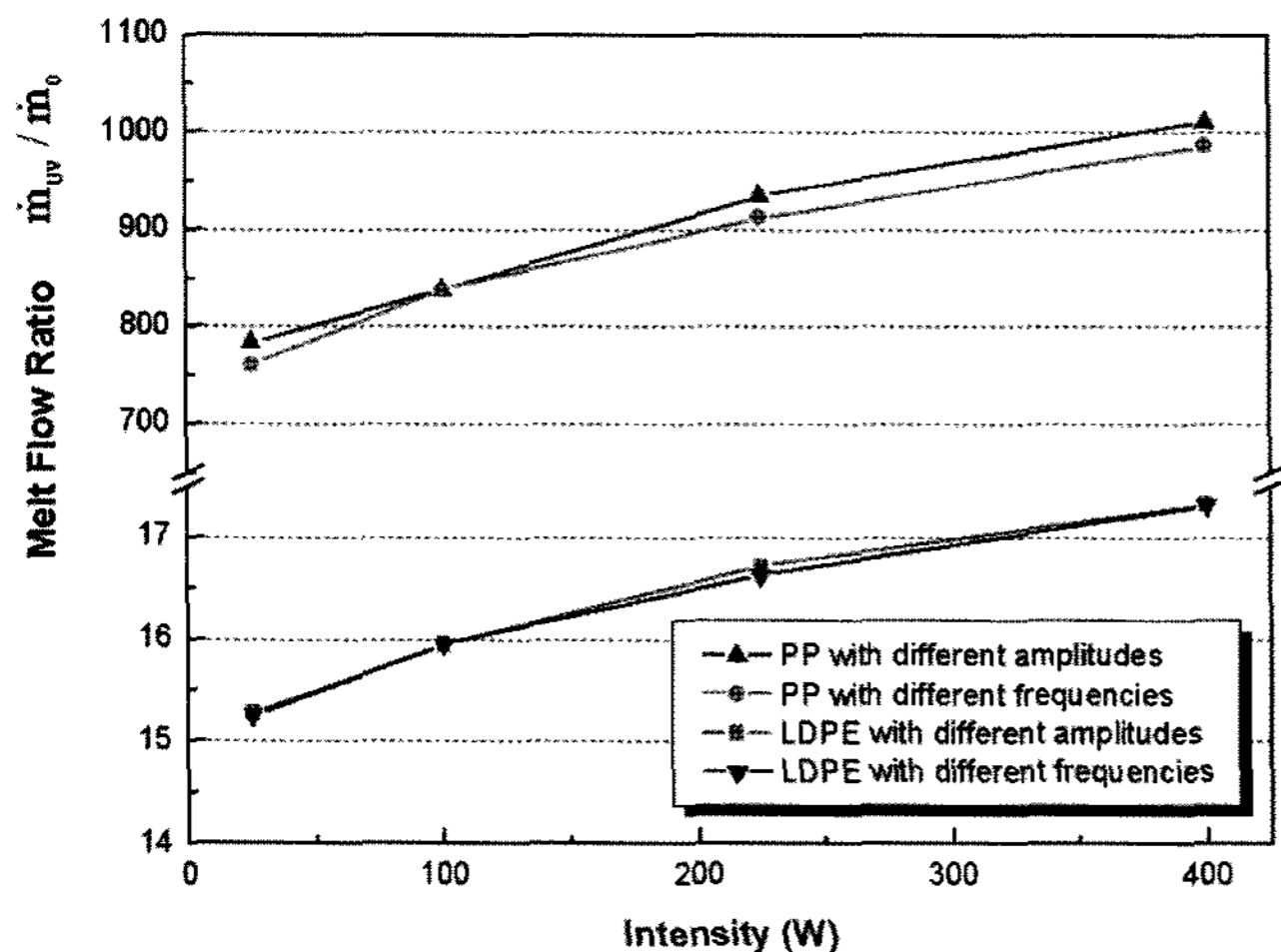


Fig. 10. Comparison of MFR according to various frequencies and amplitudes of vibration.

only the amplitude can be controlled whereas the applied frequency is fixed to adjust the intensity. As shown in equation (1), the vibrational energy, caused by the ultrasonic vibration, is related with the amplitude and the frequency of vibration. Therefore, the relationship between the frequency and the amplitude of vibration must be analyzed in equation (1).

Fig. 10 shows MFR according to the variations of the frequency and the amplitude of vibration. We considered the vibration conditions in which two opposing cavity surfaces in the y-direction, including the vibration region, as shown in Fig. 5, vibrate with the phase difference  $180^\circ$ . In the cases of both LDPE and PP, the filling efficiencies increased with the increase of the vibration intensity. At the same vibration intensity, there was little or no difference of MFR between variations of frequency and amplitude. Therefore, in theory, both the frequency and the amplitude of vibration have the same effect on the flow characteristics of polymer melt.

This conclusion about the frequency was not valid in an actual ultrasonic process because the control of only the frequency also caused the variation of the amplitude due to the changed mode shapes of the ultrasonic horn as well as the mold. On the other hand, the variation of only the amplitude had no effect on the applied frequency.

## 5.2. CASE I: Flow characteristics according to the positions of vibrating cavity surfaces

The variation of MFR according to the positions of vibrating cavity surfaces is shown in Fig. 11. It was compared with the filling efficiency in the cases of cavity surfaces in the x-direction and y-direction. The phase difference of vibration between two opposing cavity surfaces was  $180^\circ$ . The filling efficiency increased with the increase of the vibration intensity. When the cavity surfaces were applied in the y-direction, the filling efficiency

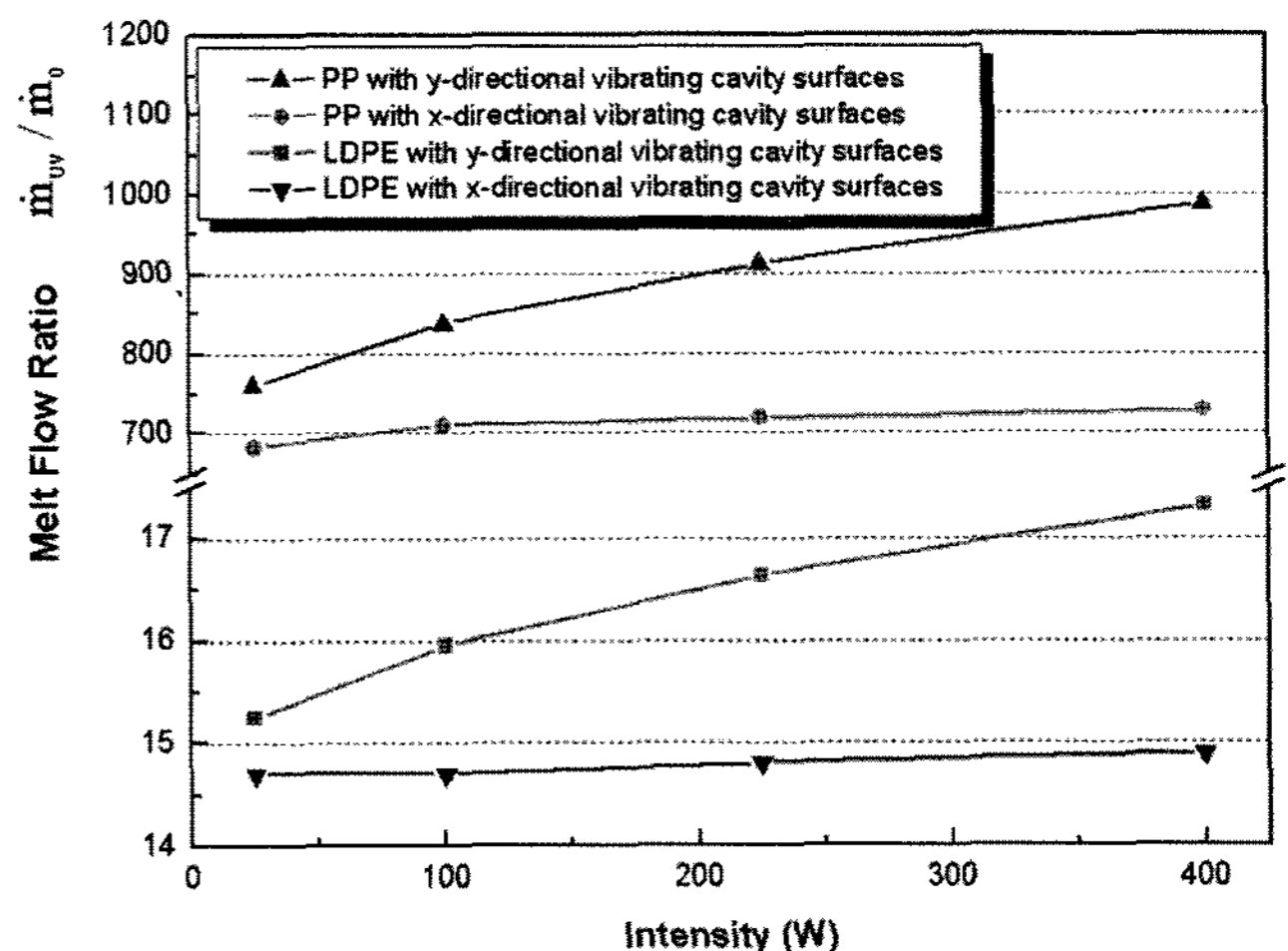


Fig. 11. Comparison of MFR according to the positions of vibrating cavity surfaces.

was higher than when cavity surfaces were applied in the x-direction. In other words, the filling efficiency insignificantly increased with the increase of the vibration intensity as the cavity surfaces in the x-direction vibrated. Considering the decrease of the filling efficiency due to the increase of the thickness as shown in Fig. 9, this reason is due to the fact that the two opposing cavity surfaces in the y-direction have larger areas and a shorter gap than in the x-direction. Depending on the polymer melt material, the filling efficiency of PP was higher than that of LDPE.

With respect to the positions of vibrating cavity surfaces, the cavity surfaces in the y-direction was a more efficient condition than the cavity surfaces in the x-direction because of the larger areas and shorter gap between two opposing cavity surfaces.

Fig. 12 shows the variations of the viscosity according to various vibration intensities when the cavity surfaces in the y-direction are applied with vibrations having the phase

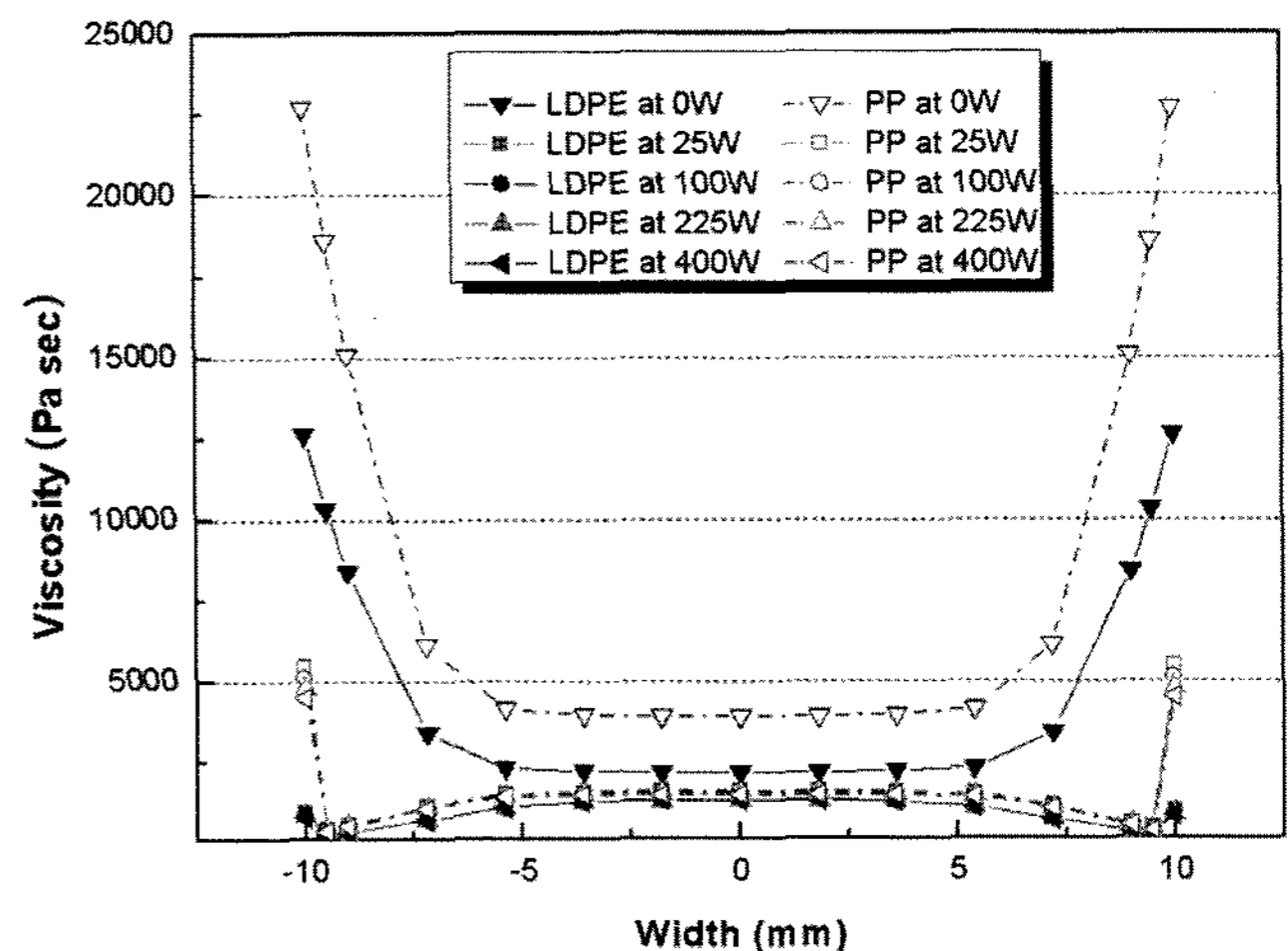


Fig. 12. Comparison of the viscosity according to various intensities.

difference 180°. These results are shown on the A-A' line of Fig. 5.

When the same vibration intensity was applied, the overall viscosity value of LDPE was lower than that of PP. In addition, the viscosity around the cavity surfaces increased due to the effect of the relatively cool temperature at the surfaces and flow resistance. In other words, high viscosity values around the cavity surfaces were obtained because of high shear forces.

Depending on the polymer melt material, the filling efficiency is related to the viscosity characteristics of polymer melt. As shown in Fig. 12, the viscosity decrease of PP, caused by the ultrasonic vibration, is higher than that of LDPE. In other words, the filling efficiency of the low viscosity material such as PP is higher than that of the high viscosity material such as LDPE due to the difference of the viscosity decrease between materials.

On the other hand, the viscosity value decreased with the increase of the vibration intensity, a phenomenon more

obvious around the cavity surfaces than in the middle of the cross section in the flow direction owing to the effect of vibrating surfaces.

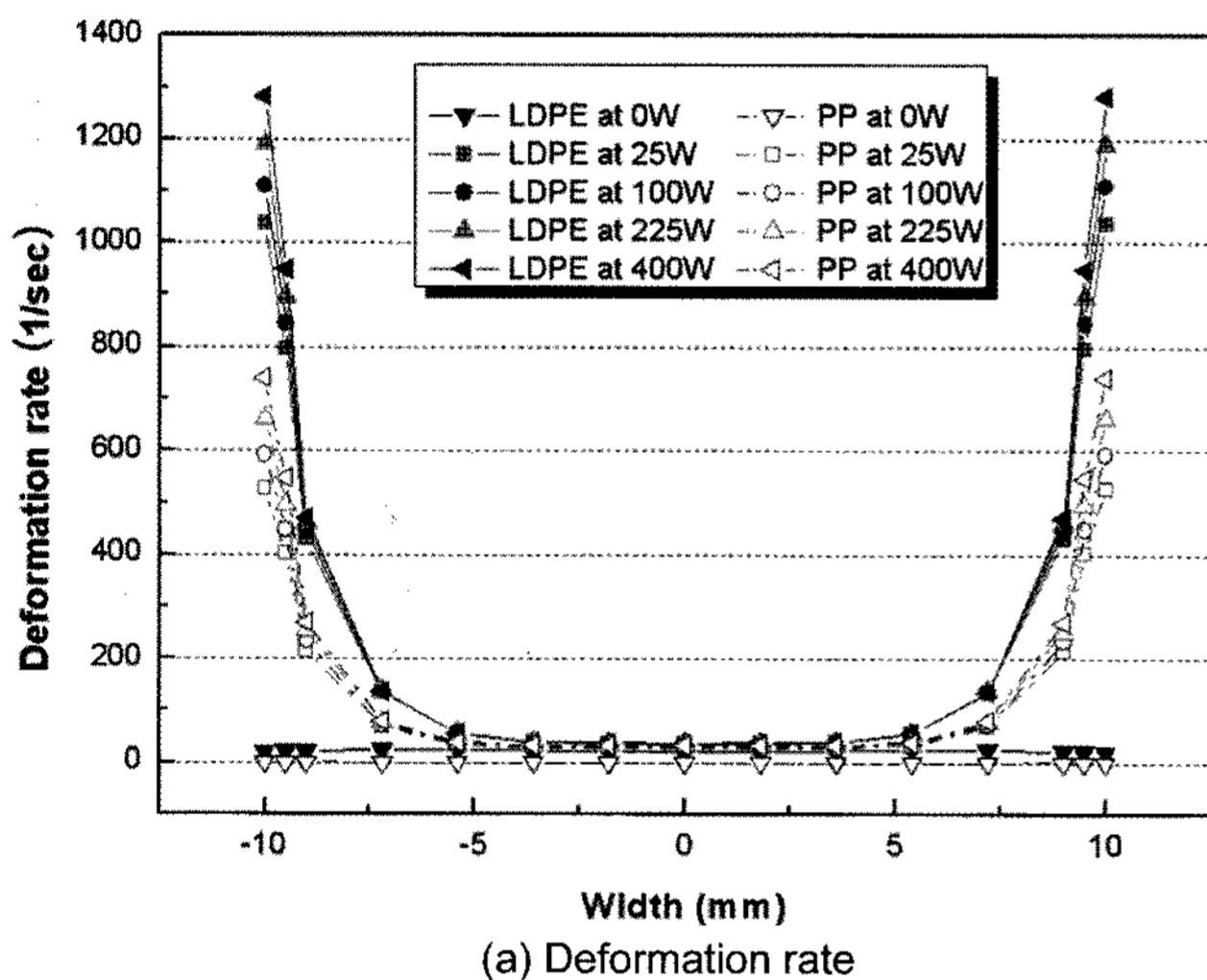
The comparison between the deformation rate and the shear rate is shown in Fig. 13. Both values of the deformation rate and the shear rate increase with the increase of the vibration intensity. There is little difference between two values, as shown in Fig. 13 (a) and (b). Considering equation (7), the deformation rate is expressed as a function of elongation rate and shear rate. The primary factor increasing the deformation rate is not the elongation rate but the shear rate. In other words, polymer melt is affected by high shear force owing to the generation of vibrations on the cavity surfaces, caused by the ultrasonic vibration. As a result of this shear force, the high shear rate increased the deformation rate. As shown in equation (6), this high deformation rate reduced the viscosity. Consequently, this low viscosity resulted in the increase of the filling efficiency.

### 5.3. CASE II: Flow characteristics according to the phase difference of vibration between two opposing cavity surfaces

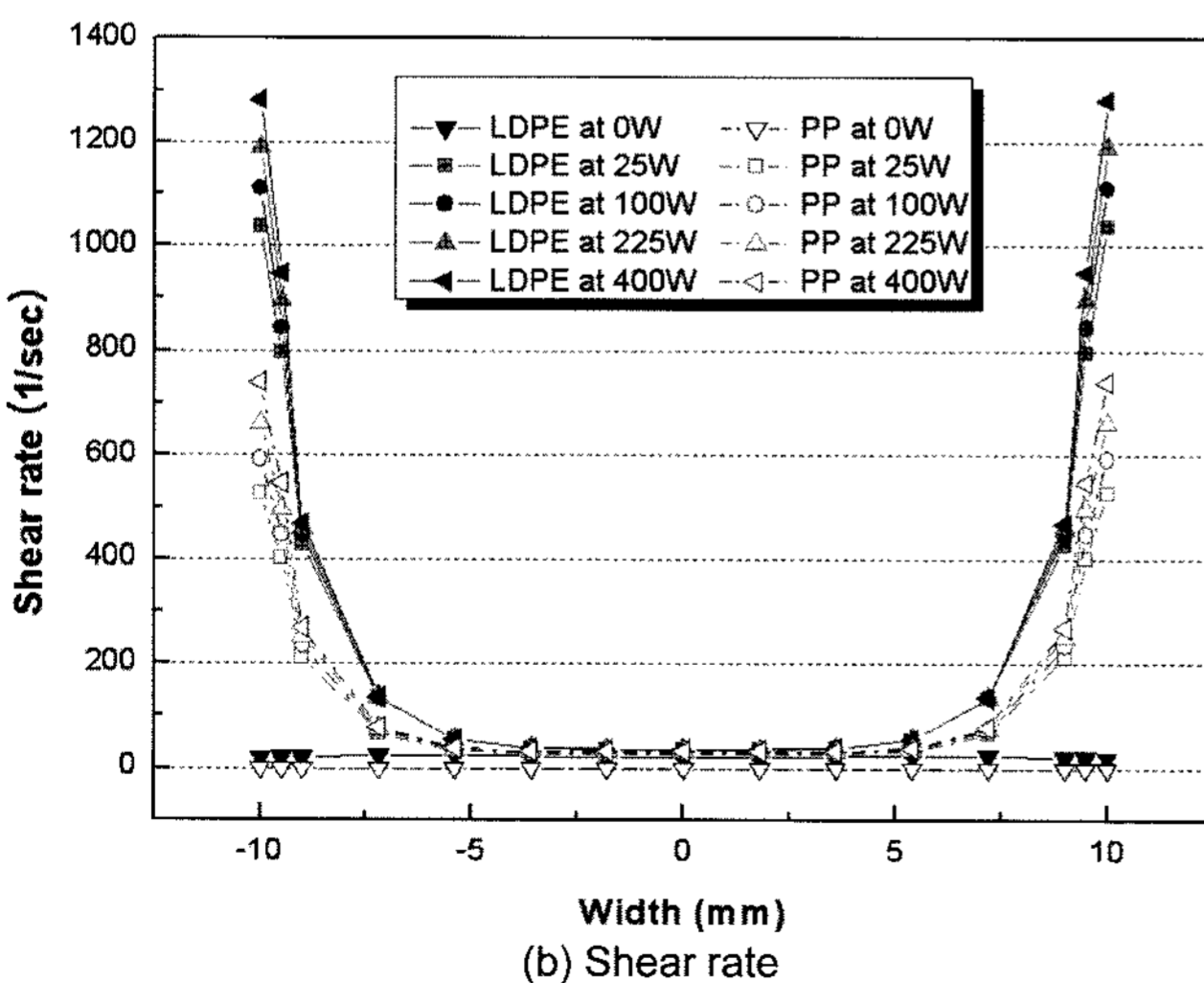
MFR according to the phase difference of vibration between two opposing cavity surfaces is shown in Fig. 14. We considered that the two opposing cavity surfaces in the y-direction were vibrated with the phase difference 180°.

The MFR with vibration of the phase difference 180° was higher than that of the phase difference 0°. In particular, while the MFR with vibration of the phase difference 180° remarkably increased with the increase of intensity, the increase of MFR with vibration of the phase difference 0° was small.

To analyze the flow characteristics of polymer melt in CASE II, the variation of the viscosity around the cavity surfaces according to the vibration intensity was investigated, as shown in Fig. 15. When vibration of the phase



(a) Deformation rate



(b) Shear rate

Fig. 13. Comparison of (a) the deformation rate and (b) the shear rate according to the intensity of vibrations.

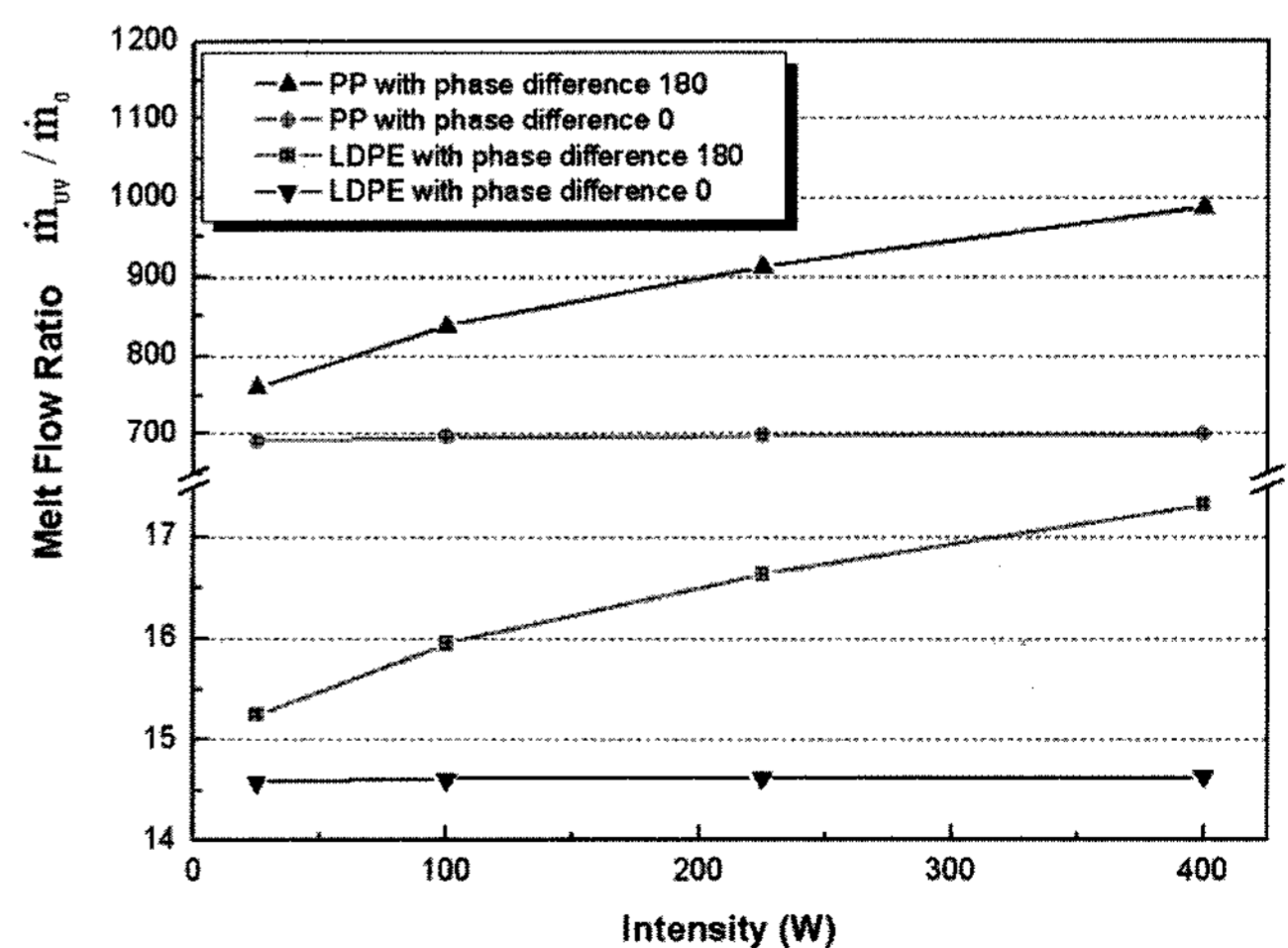


Fig. 14. Variation of MFR according to the phase difference between two opposing cavity surfaces.



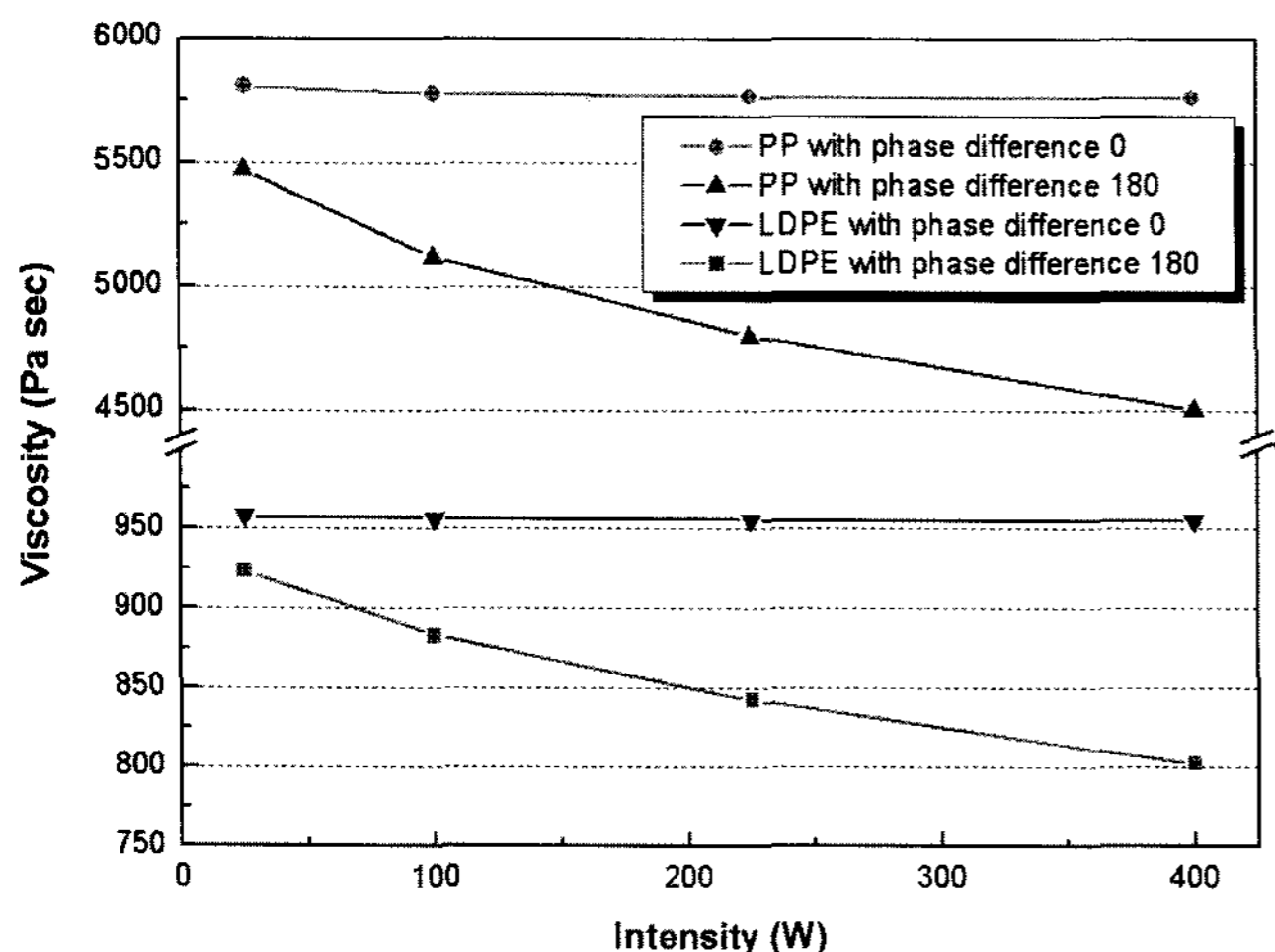


Fig. 15. Comparison of the viscosity according to the phase difference between two opposing cavity surfaces.

difference  $180^\circ$  was applied, the viscosity values of both LDPE and PP significantly decreased. On the other hand, there were little or no decrease of the viscosity values when vibration of the phase difference  $0^\circ$  was applied.

The primary physical difference between vibrations of the phase difference  $0^\circ$  and  $180^\circ$  was the variation of the flow cross section. While there was no variation of the flow cross section in vibration region with vibration of the phase difference  $0^\circ$ , the flow cross section was changed with vibration of the phase difference  $180^\circ$  because of the phase difference of vibration between two opposing cavity surfaces. As a result of this variation of the flow cross section, the decrease of the viscosity with vibration of the phase difference  $0^\circ$  was only affected by the vibration itself on the cavity surfaces, caused by the ultrasonic vibration. On the other hand, the two opposing cavity surfaces with vibration of the phase difference  $180^\circ$  caused not only this vibration itself on the cavity surfaces, but also the variation of the flow cross section. As a result, these two primary factors influenced the decrease of the viscosity when the two opposing cavity surfaces vibrated with the phase difference  $180^\circ$ . As shown in Fig. 15, this effect of the flow cross section reduced the viscosity rather than the generation of the vibration itself on the cavity surfaces. This reason is that this periodic variation of the flow cross section pushed polymer melt out of the cavity like a pump.

In conclusion, two opposing cavity surfaces vibrating with the phase difference  $180^\circ$  presented a more efficient condition than those vibrating with the phase difference  $0^\circ$  because of the periodic variation of the flow cross section, which influenced the flow characteristics.

Based on all the conclusions about vibration conditions, the most efficient condition was realized when the vibration region existed on two opposing cavity surfaces vibrating in the y-direction at the phase difference  $180^\circ$ . This is because low viscosity can be obtained by the effects of the

short gap between two opposing cavity surfaces and the generation of the vibration itself on the cavity surfaces as well as the periodic variation of the flow cross section.

## 6. Conclusions

We studied the application of ultrasonic vibration in the filling process of injection molding. To verify the validity of our numerical analysis in this study, we modeled the same extrusion system as the experiment by Chen and Li (2006) and compared the numerical results with the experimental data. We also presented MFR to estimate the filling efficiency and modeled a thin and wide cavity under the ultrasonic process. To find a more efficient injection condition, we considered cavity pressure, injection temperature and mold temperature. To find a more efficient vibration condition, we also considered the classification of vibration conditions (the relationship between the frequency and the amplitude of vibration, the position of vibrating cavity surfaces and the phase difference between vibrating surfaces) and analyzed the flow characteristics for various vibration intensities (25, 100, 225 and 400 W).

From the results, we obtained the following conclusions.

- 1) In the cases of LDPE and PP, while the flow rate increased with the increase of cavity pressure, MFR as indication of the filling efficiency decreased with the increase of the vibration intensity.
- 2) While the filling efficiency of PP increased with the increase of injection temperature, that of LDPE decreased.
- 3) The filling efficiencies of both PP and LDPE decreased with the increase of mold temperature. Especially, there was little increase of the filling efficiency of LDPE when the mold temperature increased above 320 K.
- 4) The filling efficiency decreased with the increase of the cavity thickness. The decrease rate of the filling efficiency varied according to the polymer melt material.
- 5) Depending on the material of the polymer melt, the filling efficiency of the low viscosity material is higher than that of the high viscosity material due to the difference of the viscosity decrease between materials.
- 6) With respect to vibration conditions, the most efficient condition was realized when two opposing cavity surfaces at a short gap were vibrated with the phase difference  $180^\circ$ .
- 7) The primary factor that gave a high deformation rate value was a high shear rate value, which, in turn, caused the low viscosity value. In other words, depending on the polymer melt material.
- 8) The two primary factors of the flow characteristics were the generation of the vibration itself on the cavity surfaces and the variation of the flow cross section due to the phase difference between two opposing

cavity surfaces. In particular, this variation of the flow cross section, which acted like a pump, improved the filling efficiency.

## Acknowledgments

This work was supported by Korean Research Foundation Grant (KRF-2002-005-D00010).

## Nomenclatures

$I$	: Vibration intensity
$c$	: Propagating velocity of the ultrasonic vibration
$f$	: Frequency of the ultrasonic vibration
$x$	: Amplitude of the ultrasonic vibration
$A$	: Constant
$t$	: Time
$x_j$	: Cartesian coordinate ( $j=1, 2, 3$ )
$u_i$	: Velocity component in the $x_j$ -direction
$u, v, w$	: Velocity components in the $x$ -, $y$ -, $z$ - directions, respectively
$p$	: Pressure
$T$	: Temperature
$T_{ref}$	: Reference temperature
$n$	: Power-law index
$s_m$	: Mass source term
$s_i$	: Momentum source term
$s_h$	: Energy source term
$h$	: Enthalpy
$F_{h,j}$	: Diffusional energy flux in the $x_j$ -direction
$s_{ij}$	: Strain rate tensor

## Greek symbols

$\rho$	: Density
$\tau_{ij}$	: Stress tensor components
$\mu$	: Viscosity
$\mu_0$	: zero shear viscosity
$\alpha$	: Temperature shift factor
$\dot{\gamma}$	: Deformation rate
$\lambda$	: Time constant
$\beta$	: Temperature sensitivity
$\delta_{ij}$	: Kronecker delta

## References

- Chen, Y. and H. Li, 2007, Mechanism for effect of ultrasound on polymer melt in extrusion, *J. of Polymer Sci.* **45**, 1226-1233.
- Chen, Y. and H. Li, 2006, Effect of ultrasound on the viscoelasticity and rheology of polystyrene extruded through a slit die, *J. of Appl. Polymer Science* **100**, 2907-2911.
- Feng, W. and A. I. Isayev, 2004, In situ compatibilization of PP/EPDM blends during ultrasound aided extrusion, *Polymer* **45**, 1207-1216.
- Ho, R. M., A. C. Su and C. H. Wu, 1993, Functionalization of polypropylene via melt mixing, *Polymer* **34**, 3264-3269.
- Kanwal, F., J. J. Liggat and R. A. Pethrick, 2000, Ultrasonic degradation of polystyrene solutions, *Polymer Degradation and Stability* **68**, 445-449.
- Kim, N. S., H. B. Kim and J. W. Lee, 2006a, Numerical analysis of internal flow and mixing performance in polymer extruder I: single screw element, *Korea-Australia Rheol. J.* **18**, 143-151.
- Kim, N. S., H. B. Kim and J. W. Lee, 2006b, Numerical analysis of internal flow and mixing performance in polymer extruder II: twin screw element, *Korea-Australia Rheol. J.* **18**, 153-160.
- Kim, H. S., J. G. Ryu and J. W. Lee, 2002, Evolution of phase morphology and in-situ compatibilization of polymer blends during ultrasound-assisted melt mixing, *Korea-Australia Rheol. J.* **14**, 121-128.
- Koo, M. S., K. S. Chung and J. R. Youn, 2001, Reaction injection molding of polyurethane foam for improved thermal insulation, *Polymer Eng. and Sci.* **41**, 1177-1186.
- Li, J., S. Guo and X. Li, 2005, Degradation kinetics of polystyrene and EPDM melts under ultrasonic irradiation, *Polymer Degradation and Stability* **89**, 6-14.
- Madras, G., S. Kumar and S. Chattopadhyay, 2000, Continuous distribution kinetics for ultrasonic degradation of polymers, *Polymer Degradation and Stability* **60**, 73-78.
- Morii, T., N. Ikuta and H. Hamada, 1999, Influence of ultrasonic vibration frequency on acceleration of hydrothermal aging of FRP, *J. of Thermoplastic Composite Materials* **12**, 465-476.
- Mousavi, S. A. A. A., H. Feizi and R. Madoliat, 2007, Investigations on the effects of ultrasonic vibrations in the extrusion process, *J. of Materials Processing Tech.* **187-188**, 657-661.
- Park, H., C. J. Kim and J. R. Youn, 1995, Bubble growth analysis in ultrasonic foaming using reaction injection molding, *The Korean J. of Rheol.* **7**, 237-249.
- Price, G. J., E. J. Lenz and C. W. G. Ansell, 2002, The effect of high-intensity ultrasound on the ring-opening polymerization of cyclic lactones, *European Polymer J.* **38**, 1753-1760.
- Sahnoune, A. and L. Piche, 1998, Ultrasonic study of anharmonicity in amorphous polymers: temperature, pressure and molecular weight effects, *J. of Non-Crystalline Solids* **235-237**, 664-669.
- Shim, S. E., S. Ghose and A. I. Isayev, 2002, Formation of bubbles during ultrasonic treatment of cured poly(dimethyl siloxane), *Polymer* **43**, 5535-5543.
- Swain, S. K. and A. I. Isayev, 2007, Effect of ultrasound on HDPE/clay nanocomposites: Rheology, structure and properties, *Polymer* **48**, 281-289.
- Ye, Y. S., H. B. Kim, N. Kim and J. W. Lee, 2005, A study on analysis of polymer extruder process using finite element method, *The Korean Society of Mech. Eng., Part A* **29**(1), 145-155.
- Youn, J. R., 1999, Bubble growth in reaction injection molded parts foamed by ultrasonic excitation, *Polymer Eng. and Sci.* **39**, 457-468.
- Zhang, Y., J. Chen and H. Li, 2006, Functionalization of polyolefins with maleic anhydride in melt state through ultrasonic initiation, *Polymer* **47**, 4750-4759.